

Measurement of the direct energy gap of coherently strained $\text{Sn}_x\text{Ge}_{1-x}/\text{Ge}(001)$ heterostructures

Regina Ragan^{a)} and Harry A. Atwater

Thomas J. Watson Laboratory of Applied Physics, California Institute of Technology, Pasadena, California 91125

(Received 29 December 1999; accepted for publication 20 September 2000)

The direct energy gap has been measured for coherently strained $\text{Sn}_x\text{Ge}_{1-x}$ alloys on Ge(001) substrates with $0.035 < x < 0.115$ and film thickness 50–200 nm. The energy gap determined from infrared transmittance data for coherently strained $\text{Sn}_x\text{Ge}_{1-x}$ alloys indicates a large alloy contribution and a small strain contribution to the decrease in direct energy gap with increasing Sn composition. These results are consistent with a deformation potential model for changes in the valence and conduction band density of states with coherency strain for this alloy system. © 2000 American Institute of Physics. [S0003-6951(00)03347-7]

The $\text{Sn}_x\text{Ge}_{1-x}$ binary alloy is an interesting material system due to the potential for monolithic integration of a tunable direct energy gap material with Si(001). Although growth of $\text{Sn}_x\text{Ge}_{1-x}$ is complicated by a limited bulk solid solubility, $x < 0.005$, and a tendency for Sn surface segregation due to a lower Sn surface free energy than Ge, nonequilibrium growth via molecular beam epitaxy can yield supersaturated solid solutions and Sn surface segregation can be controlled with low growth temperatures, $T < 180^\circ\text{C}$.^{1,2} Previously it was demonstrated that homogeneous, strain-relieved $\text{Sn}_x\text{Ge}_{1-x}$ epitaxial films grown on Si(001) undergo an indirect to direct energy gap transition near $x = 0.09$ yielding the first known example of a direct energy gap group IV semiconductor.³ The direct energy gap varies from $0.35 < E_g < 0.80$ for composition range $0.15 < x < 0$ for these $\text{Sn}_x\text{Ge}_{1-x}$ alloy solid solutions. The lattice mismatch for a $\text{Sn}_{0.1}\text{Ge}_{0.9}$ alloy on Si(001) is 5.7%, which is larger than for Ge on Si(001) making coherent epitaxial growth difficult. Since the presence of strain-relieving dislocations is unfavorable for optoelectronic device performance, it is desirable to know the properties of coherent $\text{Sn}_x\text{Ge}_{1-x}$ alloys. In this letter, we describe the properties of coherently strained $\text{Sn}_x\text{Ge}_{1-x}$ alloys on Ge(001) with $0.03 < x < 0.115$ and film thickness ranging between 50 and 200 nm. Advances in substrate engineering using techniques such as wafer bonding and laser liftoff⁴ may enable synthesis of dislocation-free Ge layers on Si that can serve as low cost substrates for pseudomorphic $\text{Sn}_x\text{Ge}_{1-x}$ alloy growth.

Ge buffer layers were grown by molecular beam epitaxy on (2×1) reconstructed Ge(001) substrates at $T = 450^\circ\text{C}$ in order to obtain a smooth surface, as determined by *in situ* reflection high energy electron diffraction, prior to $\text{Sn}_x\text{Ge}_{1-x}$ alloy growth. The final thickness of the Ge buffer layer was between 35 and 100 nm. During Ge buffer layer growth, the substrate temperature was lowered to the $\text{Sn}_x\text{Ge}_{1-x}$ alloy growth temperature of $T = 120\text{--}150^\circ\text{C}$. The growth rate for samples with $x < 0.06$ was $R_G = 0.05$ nm/s; for $0.07 < x < 0.115$, $R_G = 0.04$ nm/s; and for $x = 0.115$, $R_G = 0.03$ nm/s. RHEED patterns indicated that the $\text{Sn}_x\text{Ge}_{1-x}$ films are epi-

taxial and single crystalline with atomically rough surfaces. Atomic force microscopy of $500\text{ nm} \times 500\text{ nm}$ regions on 100 nm $\text{Sn}_x\text{Ge}_{1-x}$ films yielded a root-mean-square roughness of 1.1 nm for samples with $x < 0.06$ and a rms roughness of 1.5 nm for $x > 0.06$.

The crystal quality and composition have been further analyzed with high resolution x-ray diffraction and Rutherford backscattering spectroscopy. In Fig. 1(a), representative backscattering spectra taken with 2 MeV He^{++} and the sample tilted 7 degrees to the beam direction are shown for 100 nm $\text{Sn}_x\text{Ge}_{1-x}$ alloy films with $x = 0.035$, 0.06, and 0.115. The constant height of the Sn backscattering peak demonstrates the films are uniform in composition with depth and free of Sn surface segregation. The Sn composition did vary laterally over a $2\text{ cm} \times 2\text{ cm}$ region on the sample surface by $\pm 5\%$ due to a variation of Sn flux across the wafer resulting from the fixed position of the Sn effusion cell with respect to the substrate. A representative x-ray diffraction $\omega - 2\theta$ scan around the (004) reflection is shown in Fig. 1(b) for $x = 0.06$. Comparison of the experimental results for the $\text{Sn}_{0.06}\text{Ge}_{0.94}$ alloy film with a dynamical simulation generated using the Takagi-Taupin equations⁵ confirms the backscattering composition of $x = 0.06$. The finite thickness interference fringes yield a value of 99 nm for the film thickness and indicate the absence of strain relaxation at the $\text{Sn}_x\text{Ge}_{1-x}/\text{Ge}$ interface. Assuming the linear relationship between composition and lattice parameter that has been shown to hold experimentally for the $\text{Sn}_x\text{Ge}_{1-x}$ alloy system,³ the strain parallel to the growth direction, e_{zz} , and in the plane of the substrate surface, e_{xx} , are calculated as a function of Sn composition⁶ and are illustrated as the solid lines in Fig. 1(c). The angular displacement of the $\text{Sn}_x\text{Ge}_{1-x}$ (004) reflection from the Ge(004) reflection yields the lattice constant along the growth direction from which e_{zz} can be calculated. The angular displacement of the $\text{Sn}_x\text{Ge}_{1-x}$ (224) asymmetric reflection with respect to the Ge(224) reflection is deconvoluted to determine e_{xx} . The experimental results for e_{zz} and e_{xx} , represented by triangles and squares in Fig. 1(c), respectively, are in agreement with predictions for pseudomorphic $\text{Sn}_x\text{Ge}_{1-x}$ epitaxial films on Ge(001).

^{a)}Electronic mail: regina@its.caltech.edu

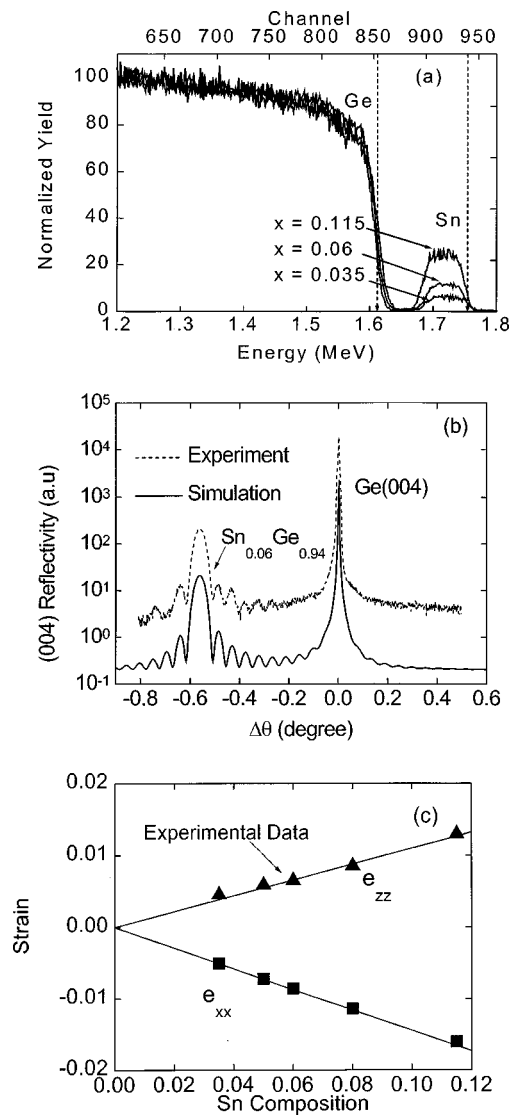


FIG. 1. In (a), Rutherford backscattering spectra of 100 nm Sn_xGe_{1-x}/Ge(001) films with the sample tilted 7° to the beam direction for $x = 0.035, 0.06,$ and 0.115 . In (b), representative high resolution x-ray diffraction $\omega - 2\theta$ scan of 100 nm Sn_{0.06}Ge_{0.94}/Ge(001) films around the Ge(004) reflection (dashed curve) overlaid with dynamical simulation (solid curve). In (c), comparison between calculated (solid lines) and experimentally measured strains along the growth direction, e_{zz} (triangles), and in the substrate plane, e_{xx} (squares), for 100 nm coherently strained Sn_xGe_{1-x} films on Ge(001).

The thickness and composition constraints to growth of coherently strained films were investigated and compared to simple models for the critical thickness for misfit dislocation generation. From x-ray diffraction measurements, Sn_xGe_{1-x} alloy films with $0.035 < x < 0.115$ with film thickness up to 219 nm were determined to be pseudomorphic on Ge(001). These pseudomorphic thicknesses substantially exceed the critical thickness predicted by the Matthews–Blakeslee model.⁷ For instance, a Sn_xGe_{1-x} alloy film with $x = 0.078$ and film thickness of 155 nm is coherently strained, whereas the Matthews–Blakeslee model predicts a critical thickness of 9.3 nm. Growth of metastably strained, coherent epitaxial films is consistent with previous reports from other strained, semiconductor alloys, such as the Si_{1-x}Ge_x system. For Si_{1-x}Ge_x heterostructures, a kinetic phenomenological model yields stress-temperature diagrams where the amount

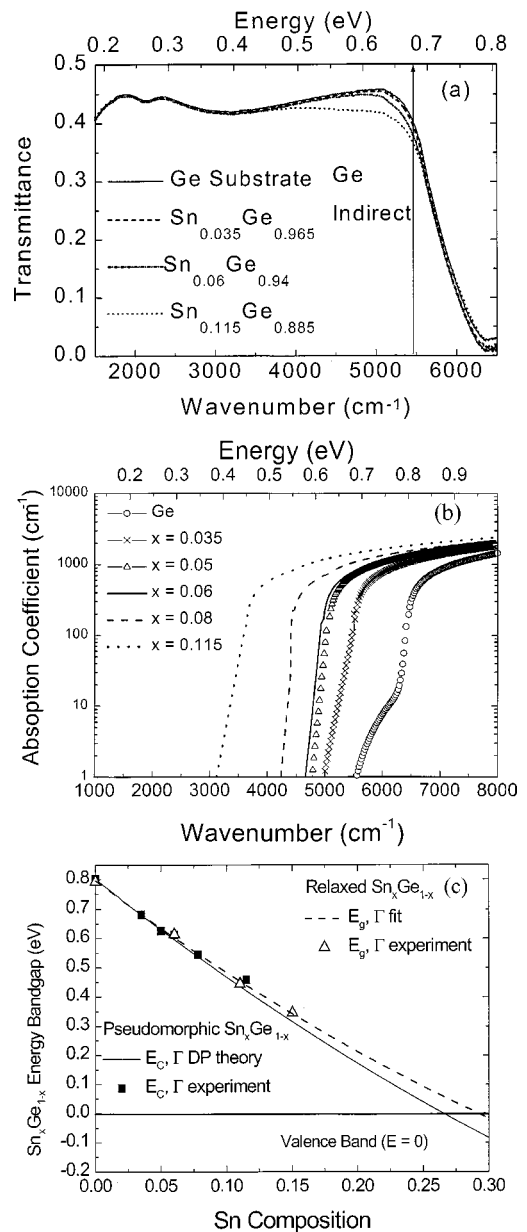


FIG. 2. In (a), infrared transmittance of 100 nm Sn_xGe_{1-x} alloys on *p*-type Ge(001) for $x = 0.035, 0.06, 0.115$. In (b), absorption coefficient vs wave number used in simulated transmittance curves having best fit with experimental curves. In (c), comparison of Sn_xGe_{1-x} alloy direct energy gaps for pseudomorphic and strain-relieved films. Open triangles are experimental values of the direct energy gap for strain relieved alloys; dashed curve is a fit to these data; solid squares are experimental values for coherently strained Sn_xGe_{1-x} alloys on Ge(001); solid line is the direct energy gap predicted by deformation potential theory.

of strain relaxation is small, $< 10^{-7}$, at low temperatures, $T < 0.5T_m$.⁶ Since the Sn_xGe_{1-x} epitaxial films are dilute alloys grown at temperatures, $T < 150^\circ\text{C}$, much less than $0.5T_m$ for Ge, the nucleation rate for misfit dislocations is expected to be low leading to the observed negligible dislocation density.

In order to characterize the effect of strain on the energy gap, infrared transmittance, depicted in Fig. 2(a), and reflectance measurements were performed using a Fourier transform infrared spectrometer between 1000 and 8000 cm⁻¹ at 300 K. Reflectance measurements demonstrate a monotonic increase in the refractive index with Sn content in agreement with previous reports.³ Transmittance versus wave number

was simulated between 3000 and 8000 cm^{-1} using a functional form of the absorption coefficient that includes direct transitions, indirect transitions, and transitions between bandtails using values of the band gap predicted by deformation potential theory calculations.⁸

Deformation potential theory predicts that the unit cell dilation increases the energy gap while the uniaxial splitting of the valence band increases the energy of the heavy hole valence band, decreasing the energy gap. The net effect is a small decrease in the energy gap for coherently strained films relative to strain-relieved films. The details of calculations supporting this conclusion are described elsewhere.⁸ In order to compare the experimental value of the band gap with deformation potential theory calculations, the root-mean-square error was minimized between the simulated and experimental transmittance data by iteratively fitting the direct band gap, the indirect band gap, and the Urbach tail. The best fit of the absorption coefficient versus wave number is seen in Fig. 2(b). Figure 2(c) illustrates the decrease in the direct energy gap with increasing strain. The dotted curve in Fig. 2(c) is a fit to the experimental energy gap (open triangles) for unstrained alloys. At $x=0.08$, the experimentally measured energy gap is 0.55 eV for coherently strained alloys (solid squares) versus 0.549 eV for the strain-relieved alloys; the energy difference is negligible in comparison to the experimental error in the measurements. The small strain induced

decrease in the direct energy gap predicted with deformation potential calculations for strained pseudomorphic $\text{Sn}_x\text{Ge}_{1-x}$, depicted as the solid curve in Fig. 2(c) is not resolvable in transmittance measurements. The uniaxial splitting of the valence band, ΔE_V , is evident in transmittance measurement in that the density of states is reduced to the heavy hole contribution between E_g , Γ , and E_g , $\Gamma + \Delta E_V$ to obtain the best fit to the experimental transmittance data for $x > 0.07$. In summary, the direct energy band gap of $\text{Sn}_x\text{Ge}_{1-x}$ alloys decreases primarily through an increase in alloy concentration in this system. The effect of coherency strain on the $\text{Sn}_x\text{Ge}_{1-x}$ alloy band gap is evident in a reduction in the valence band density of states rather than a reduction of the magnitude of the energy band gap.

- ¹P. R. Pukite, A. Harwit, and S. S. Iyer, *Appl. Phys. Lett.* **52**, 2142 (1989).
- ²O. Gurdal, P. Desjardins, R. A. Carlsson, N. Taylor, H. H. Radamson, J. E. Sundgren, and J. E. Greene, *J. Appl. Phys.* **83**, 162 (1998).
- ³G. He and H. Atwater, *Phys. Rev. Lett.* **79**, 1937 (1997).
- ⁴W. S. Wong, T. Sands, N. W. Cheung, M. Kneissl, D. P. Bour, P. Mei, L. T. Romano, and N. M. Johnson, *Appl. Phys. Lett.* **75**, 1360 (1999).
- ⁵M. Wormington, C. Panaccione, K. M. Matney, and D. K. Bowen, *Philos. Trans. R. Soc. London, Ser. A* **357**, 2827 (1999).
- ⁶J. Y. Tsao, *Material Fundamentals of Molecular Beam Epitaxy* (Academic, New York, 1993).
- ⁷J. W. Matthews and A. E. Blakeslee, *J. Cryst. Growth* **27**, 118 (1974).
- ⁸R. Ragan and H. A. Atwater, *Mater. Res. Soc. Symp. Proc.* **588**, 199 (1999).